

Crystallization and preliminary X-ray analysis of the thymidylate kinase from *Mycobacterium tuberculosis*I. Li de la Sierra,<sup>a\*</sup> H. Munier-Lehmann,<sup>b</sup> A. M. Gilles,<sup>b</sup> O. Bárzu<sup>b</sup> and M. Delarue<sup>a</sup><sup>a</sup>Unité de Biochimie Structurale, Institut Pasteur, 28 Rue du Dr Roux, 75724, Paris CEDEX 15, France, and <sup>b</sup>Laboratoire de Chimie Structurale des Macromolécules, Institut Pasteur, 28 Rue du Dr Roux, 75724, Paris CEDEX 15, France

Correspondence e-mail: ines@pasteur.fr

*Mycobacterium tuberculosis* thymidylate kinase complexed with the substrate deoxythymidine monophosphate was crystallized in the hexagonal space group  $P6_522$  or  $P6_122$ , with unit-cell parameters  $a = b = 76.62$ ,  $c = 134.38$  Å and one single monomer of 23 kDa in the asymmetric unit. Cryo-cooled crystals diffract at 1.94 Å resolution using synchrotron radiation.

Received 22 October 1999  
Accepted 9 December 1999

### 1. Introduction

Thymidylate kinase (E.C. 2.7.4.9; ATP:dTMP phosphotransferase; TMPK) belongs to the nucleoside monophosphate kinase (NMPK) family and catalyzes the phosphorylation of deoxythymidine monophosphate (dTMP) to deoxythymidine diphosphate (dTDP) using ATP as the phosphoryl donor in both *de novo* and salvage pathways of dTTP synthesis. Being essential for DNA synthesis and cellular growth (Anderson, 1973; Neuhard & Nygaard, 1996), this enzyme appeared to be an attractive target for the development of drugs against cancer (Jong & Campbell, 1984) and various viruses (Griffith, 1995; Darby, 1995). Variability in the structure and catalytic properties of TMPKs from various sources opened the possibility of designing specific inhibitors. Such inhibitors of *M. tuberculosis* thymidylate kinase (TMPK<sub>mt</sub>) might be effective agents in limiting the spread of tuberculosis.

The three-dimensional structures of the NMPK family display a similar general topology. Nevertheless, several conformational changes can occur depending upon the occupancy of each of the nucleotide-binding sites (Vonnrhein *et al.*, 1995; Lavie *et al.*, 1997; Briozzo *et al.*, 1998). A high variability in the local structure and catalytic properties of this family of proteins was also observed (Brown *et al.*, 1995; Lavie *et al.*, 1997; Lavie, Konrad *et al.*, 1998; Lavie, Ostermann *et al.*, 1998; Chenal-Francois *et al.*, 1999). The three-dimensional structures of TMPKs from yeast and *Escherichia coli* have been solved recently at high resolution (Lavie *et al.*, 1997; Lavie, Konrad *et al.*, 1998; Lavie, Ostermann *et al.*, 1998) and their analysis led the authors to propose a classification of TMPKs into two types according to the sequence variability of the catalytic region containing the phosphate binding loop (P-loop) and the region which covers part of the phosphate donor binding site (LID). The TMPK<sub>mt</sub> sequence, however,

departs from both types in these two regions when compared with both yeast and *E. coli* enzymes. Moreover, the TMPK<sub>mt</sub> kinetic properties show significant differences to the other two enzymes (Munier-Lehmann *et al.*, 2000). In order to explain these differences, we have crystallized the recombinant TMPK<sub>mt</sub> in complex with dTMP and report here its preliminary X-ray study.

### 2. Materials and methods

The *tmk* gene of *M. tuberculosis* was cloned in *E. coli* and the overexpressed protein (a dimer of 214 amino acids per monomer) was purified by chromatography on blue-Sepharose and gel filtration (Munier-Lehmann *et al.*, 2000). The purity and the identity of the protein was controlled by SDS-PAGE and electrospray ionization mass spectrometry (ESI-MS). TMPK<sub>mt</sub> was concentrated to 7–8 mg ml<sup>-1</sup> in 20 mM Tris-HCl pH 7.4, 1 mM EDTA, 0.5 mM DTT using a centrifugal filter device (Nanosep 10 K, Pallfiltron) at 277 K. This stock solution was conserved at 253 K for further crystallization experiments.

Crystallization trials were performed at 293 K by hanging-drop vapour diffusion using 24-well culture plates. Each hanging drop was prepared by mixing 3–5 µl of TMPK<sub>mt</sub>-dTMP protein solution (270–392 µM TMPK<sub>mt</sub>, 2 mM dTMP, 1 mM DTT, 2 mM EDTA, 15 mM Tris-HCl pH 7.4) with an equal volume of the reservoir solution. The drops were equilibrated against 1 ml reservoir solution.

All data were collected from cryo-cooled crystals. Single crystals of TMPK<sub>mt</sub>-dTMP were transferred using a Hampton Research loop into a stabilization solution which contained 25% glycerol. The loops were placed in a stream of nitrogen at 110 K to cryo-cool the crystal immediately prior to collecting data using an Oxford Cryosystems Cryostream or

**Table 1**  
Data-collection conditions and statistics for the different diffraction data sets.

	Nat	Nat1	EtHgPO <sub>4</sub>
X-ray source (wavelength in Å)	In-house (1.5418)	ESRF ID14-3 (0.94)	LURE (1.28)
Detector	MAR imaging plate	MARCCD	MAR imaging plate
Crystal-to-detector distance (mm)	250	120 (250)†	200
Total rotation scan‡ (°)	71	80 (80)†§	82
Exposure time (s)	1800	5 (1)†	420
Space group	<i>P</i> <sub>6</sub> ,22 or <i>P</i> <sub>6</sub> ,22	<i>P</i> <sub>6</sub> ,22 or <i>P</i> <sub>6</sub> ,22	<i>P</i> <sub>6</sub> ,22 or <i>P</i> <sub>6</sub> ,22
Unit-cell parameters			
<i>a</i> , <i>b</i> (Å)	74.92	76.62	76.84
<i>c</i> (Å)	131.28	134.38	134.98
Resolution (Å)	20–3.6	40–1.9	12–3.0
Total number of reflections	21067	184620	22643
Number of unique reflections	2799	18761	4571
Multiplicity	7.5 (7.9)	9.5 (7.1)	5.0 (4.8)
Completeness (%)	99.9 (99.9)	100 (99.9)	90.7 (91.2)
<i>R</i> <sub>merge</sub> ¶	0.131 (0.202)	0.052 (0.374)	0.094 (0.120)
<i>I</i> / <i>σ</i> ( <i>I</i> )	22.0 (14.0)	37.4 (6.95)	26.1 (19.5)
<i>R</i> <sub>iso</sub> ††	—	—	0.173

† Values for the low-resolution pass are in parentheses. ‡ All collections were carried out with an oscillation angle of 1°. § With three passages per oscillation angle. ¶  $R_{\text{merge}} = \frac{\sum_h \sum_i |I_{hi} - \langle I_h \rangle|}{\sum_h \sum_i I_{hi}}$ , where  $I_{hi}$  is the  $i$ th observation of the reflection  $h$ , while  $\langle I_h \rangle$  is the mean intensity of reflection  $h$ . ††  $R_{\text{iso}} = \frac{\sum |F_{PH} - F_P|}{\sum F_P}$ , where  $F_{PH}$  and  $F_P$  are the derivative and the native structure-factor amplitudes, respectively.

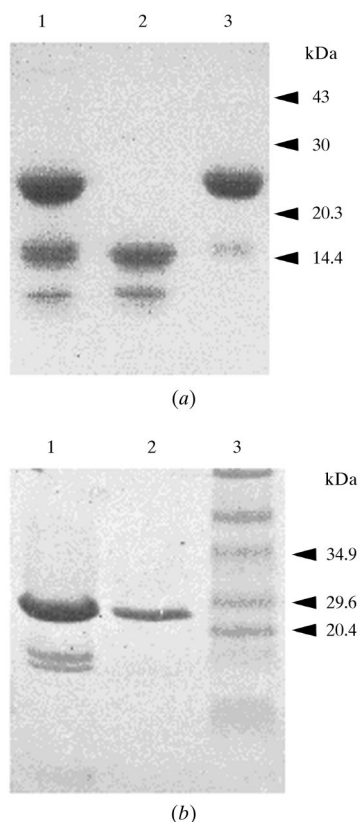


**Figure 1**  
(a) SDS-PAGE (12.5%). Pharmacia molecular-weight markers are indicated on the right. Lane 1, TMPKmt after three weeks at room temperature; lane 2, TMPKmt–dTMP complex under the same conditions; lane 3, TMPKmt–dTMP complex in presence of 1 mM EDTA and 0.5 mM DTT. (b) High Density Phast Gel (SDS, 8–25%). Lane 1, TMPKmt protein solution used for crystallization; lane 2, washed crystals of the TMPKmt–dTMP complex; lane 3, Biorad molecular-weight markers (molecular weights are indicated on the right).

were cryo-cooled and stored in liquid nitrogen for further data collection.

Several heavy-atom derivatives were screened in order to solve the structure by MIR methods. TMPKmt–dTMP crystals were soaked in the stabilization solution with increased concentration of ammonium sulfate and heavy-atom reagents.

Diffraction data from the first native and the mercury-derivative crystals were processed using the *MARXDS* package (Kabsch, 1988a,b). Data from the second native crystal were processed with the *DENZO/SCALEPACK* suite of programs (Otwinowski & Minor, 1997). The *CCP4* package (Collaborative Computational Project, Number 4, 1994) was used to calculate observed structure factors and their intensity distribution (*TRUNCATE*) and scale native data to derivative data (*FHSCAL*). The Patterson maps were interpreted with the automated procedure developed in the program *HEAVY* (Terwilliger & Eisenberg, 1987) and the heavy-atom position was refined with *MLPHARE*

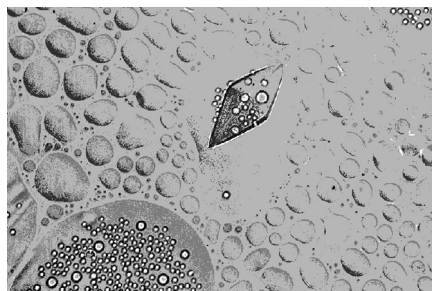


**Figure 2**  
A typical crystal of the TMPKmt–dTMP complex, measuring 0.3 mm in the longest dimension.

(*CCP4*); *DM* (*CCP4*) was used for solvent-flattening calculations.

### 3. Results and discussion

The TMPKmt was of high purity. The mass of the protein in ESI–MS of  $22\,635.89 \pm 2.23$  Da corresponds to that calculated from the sequence (22 634.58 Da) within the estimated error. Crystals of the TMPKmt–dTMP complex grown using the same reservoir solution without EDTA and reducing agent were not stable and diffracted poorly. Biochemical analysis showed that in the presence of 2 mM dTMP, TMPKmt was proteolyzed into two fragments (Fig. 1a), one corresponding to residues 1–148 (molecular mass of  $15\,507.98 \pm 1.17$  Da determined by ESI–MS). When 1 mM EDTA and 0.5 mM DTT were included in buffers used for purification of the TMPKmt (Fig. 1a) and crystallization of the TMPKmt–dTMP complex, this phenomenon was suppressed (Fig. 1b).

The best crystals were obtained with a reservoir solution consisting of 35% ammonium sulfate, 2% PEG 2000, 0.1 M MES pH 6.0, 2 mM  $\beta$ -mercaptoethanol, 25 mM magnesium acetate. Suitable TMPKmt–dTMP bipyrarnidal crystals appeared after about one month (Fig. 2) and have typical dimensions of up to  $150 \times 150 \times 300$   $\mu\text{m}$ . They belong to space group *P*<sub>6</sub>,22 or *P*<sub>6</sub>,22, with unit-cell parameters  $a = b = 76.62$ ,  $c = 134.38$  Å for the best single-crystal data set collected thus far. Assuming one TMPKmt–dTMP monomer per asymmetric unit, the volume of the asymmetric unit divided by the protein molecular weight ( $V_m$ ) value is  $2.48$  Å<sup>3</sup> Da<sup>−1</sup> and the solvent content is 50%, which is near the average values found for most protein molecules (Matthews, 1968).

A cryo-cooled TMPKmt–dTMP crystal diffracted X-rays to 3.6 or 1.9 Å using in-house and synchrotron X-ray radiation, respectively. Data were collected from two TMPKmt–dTMP native crystals (Table 1). A complete data set for a first crystal diffracting to 3.6 Å was obtained using Cu  $K\alpha$  radiation from a rotating-anode generator. Two data sets for the second crystal were collected at high (1.9 Å) and low (3.68 Å) resolution using the ESRF synchrotron-radiation facility, Grenoble.

Diffraction data from an EtHgPO<sub>4</sub> heavy-atom derivative was obtained (Table 1) at 3 Å resolution using synchrotron X-ray radiation at the LURE laboratory, Orsay. The isomorphous difference Patterson map revealed one heavy-atom site. The heavy-atom position was refined at 9–3.8 Å reso-

lution with a phasing power of 1.1 and an  $R_{\text{Cullis}}$  value of 0.86 for acentric reflections. The values of the mean figure of merit (FOM) was 0.23 before and 0.59 after phase improvement through solvent flattening. A search for additional isomorphous heavy-atom derivatives is under way.

We thank A. Namane for ESI-MS and N. Expert-Bezancon for SDS-PAGE. We thank W. Shepard and X. Perez at LURE and S. Arzt and W. Burmeister at ESRF for help with synchrotron data collection. This work was supported by a post-doctoral fellowship from the EEC and grants from the EEC, the Institut Pasteur and the Centre National de la Recherche Scientifique (URA 1129).

### References

- Anderson, E. P. (1973). *The Enzymes*, edited by P. D. Boyer, Vol. 8, pp. 49–96. New York: Academic Press.
- Briozzo, P., Golinelli-Pimpaneau, B., Gilles, A.-M., Gaucher, J.-F., Burlacu-Miron, S., Sakamoto, H., Janin, J. & Barzu, O. (1998). *Structure*, **6**, 1517–1527.
- Brown, D. G., Visse, R., Sandhu, G., Davies, A., Rizkallah, P. J., Melitz, C., Summers, W. C. & Sanderson, M. R. (1995). *Nature Struct. Biol.* **2**, 876–881.
- Chenal-Francisque, V., Tourneux, L., Carniel, E., Christova, P., Li de la Sierra, I. M., Bâzru, O. & Gilles, A.-M. (1999). *Eur. J. Biochem.* **265**, 112–119.
- Collaborative Computational Project, Number 4. (1994). *Acta Cryst. D***50**, 760–763.
- Darby, G. K. (1995). *Antivir. Chem. Chemother.* **6**, 54–63.
- Griffith, P. D. (1995). *Antivir. Chem. Chemother.* **6**, 191–209.
- Jong, A. Y. & Campbell, J. L. (1984). *J. Biol. Chem.* **259**, 14394–8.
- Kabsch, W. (1988a). *J. Appl. Cryst.* **21**, 67–71.
- Kabsch, W. (1988b). *J. Appl. Cryst.* **21**, 916–924.
- Lavie, A., Konrad, M., Brundiers, R., Goody, R. S., Schlichting, I. & Reinstein, J. (1998). *Biochemistry*, **37**, 3677–3686.
- Lavie, A., Ostermann, N., Brundiers, R., Goody, R. S., Reinstein, J., Konrad, M. & Schlichting, I. (1998). *Proc. Natl Acad. Sci. USA*, **95**, 14045–14050.
- Lavie, A., Vetter, I. R., Konrad, M., Goody, R. S., Reinstein, J. & Schlichting, I. (1997). *Nature Struct. Biol.* **4**(8), 601–604.
- Matthews, B. W. (1968). *J. Mol. Biol.* **33**, 491–497.
- Munier-Lehmann, H., Chaffotte, A. & Labesse, G. (2000). In preparation.
- Neuhard, J. & Nygaard, P. (1996). *Escherichia coli and Salmonella typhimurium: Cellular and Molecular Biology*, edited by F. C. Neidhardt, R. Curtiss, J. L. Ingraham, E. C. C. Lin, K. B. Low, B. Magasanik, W. S. Reznikoff, M. Riley, M. Schaechter & H. E. Umberger, Vol. 1, pp. 580–599. Washington DC: American Society for Microbiology.
- Otwinowski, Z. & Minor, W. (1997). *Methods Enzymol.* **276**, 307–326.
- Terwilliger, T. C. & Eisenberg, D. (1987). *Acta Cryst.* **A43**, 6–13.
- Vonrhein, C., Schlauderer, G. J. & Schulz, G. E. (1995). *Structure*, **3**, 483–490.